

# Heat and Mass Transfer Mixed Convective Electrically Conducting Nanomaterial Flow Over a Stretching Sheet

Lawal Muhammad Muhammad<sup>1</sup>

<sup>1</sup>Department of Mathematics,  
Federal University of Petroleum Resources,  
Effurun, Nigeria  
lawal.muhammad@fupre.edu.ng<sup>1</sup>

Ogboru Oghenero Kelvin<sup>2</sup>

<sup>2</sup>Department of Mathematics,  
Federal University of Petroleum Resources,  
Effurun, Nigeria  
kelogfoundation@yahoo.com<sup>2</sup>

Okedoye Akindele Michael<sup>3</sup>

<sup>3</sup>Department of Mathematics,  
Federal University of Petroleum Resources,  
Effurun, Nigeria  
okedoye.akindele@fupre.edu.ng<sup>3</sup>

**Abstract**— The study of heat and mass transfer in electrically conducting nanomaterial flows over a stretching sheet is a complex phenomenon involving fluid mechanics, thermodynamics, and electrical conductivity. The flow of electrically conducting nanomaterials over a stretching sheet is governed by the Navier-Stokes and Maxwell equations, which describe momentum and electric field distributions. The electrical conductivity of the nanomaterials plays a crucial role in the flow behavior, as it affects the electric field distribution and fluid motion. Numerical simulations using the finite volume method were conducted to investigate the effects of electrical conductivity, nanoparticle volume fraction, and stretching velocity on the flow, heat, and mass transfer characteristics. Results showed that electrical conductivity significantly impacts the flow structure, leading to the formation of electrically induced vortices and streamlines. The nanoparticle volume fraction also affects the flow behavior, increasing fluid viscosity and decreasing fluid velocity. These findings have important implications for the design and optimization of nanomaterial-based devices and processes, such as energy harvesting, water purification, and drug delivery.

**Keywords**—Magnetohydrodynamics, Nanomaterials, Stretching sheet, Heat transfer, Numerical simulations.

## I. INTRODUCTION

The study of heat and mass transfer in electrically conducting nanomaterial flows over a stretching sheet is a complex phenomenon involving fluid mechanics, thermodynamics, and electrical conductivity. The flow of electrically conducting nanomaterials over a stretching sheet is governed by the Navier-Stokes and Maxwell equations, which describe momentum and electric field distributions. The electrical conductivity of the nanomaterials plays a crucial role in the flow

behavior, as it affects the electric field distribution and fluid motion. Numerical simulations using the finite volume method were conducted to investigate the effects of electrical conductivity, nanoparticle volume fraction, and stretching velocity on the flow, heat, and mass transfer characteristics. Results showed that electrical conductivity significantly impacts the flow structure, leading to the formation of electrically induced vortices and streamlines. The nanoparticle volume fraction also affects the flow behavior, increasing fluid viscosity and decreasing fluid velocity. These findings have important implications for the design and optimization of nanomaterial-based devices and processes, such as energy harvesting, water purification, and drug delivery. Melting fluid dynamics and heat transfer are crucial in manufacturing processes, and simulation is complex due to Stefan moving boundary problems, with melting front position and Nusselt number being key variables. Computational strategies are needed for problems involving melting heat transfer; however, a more straightforward method is to simulate the melting effect as a boundary condition that is consistent with boundary layer flow models and yields precise approximations.

Nanofluids can be considered as the next-generation heat-transfer fluids, as they offer exciting new possibilities to enhance heat-transfer performance compared to pure liquids. This concept attracted various researchers to nanofluids, and various theoretical and experimental studies have been performed to find the thermal properties of nanofluids. [1] study A benchmark study of thermal conductivity of nanofluids. [2] study Flow and heat transfer of a nanofluid over a nonlinearly stretching sheet. [3] study MHD Free Convection Flow of a Nanofluid past a Vertical Plate in the Presence of Heat Generation or Absorption Effects. It is an established contention that several industrial and engineering processes involving heat and mass transport such as glass fiber, metal extrusion, rubber manufacturing, and many more takes

place in the presence of simultaneous effects of thermal and species buoyancy forces. Different studies on the fluid flow through an inclined, horizontal and vertical surface in the existence of magnetic field have been examined. [4] investigated gravity driven flow of reactive hydromagnetic fluid through a vertical channel in the presence of magnetic field. [5], [6] studied hydromagnetic reactive fluid flow through horizontal porous plates with radiation and internal heat generation. A computational solution of a convective transient fluid flow with thermal radiation over a moving plate of a Sisko binary fluid was analyzed by [7]. A few great reports on the flow of fluid through a stretching surface are presented by [8], [9], and [10]., [11] also examine effect of free convective flow is characterized by linear density difference embodies buoyant forces. [12] examined the radiation effect on the conducting flow fluid influenced by pressure and magnetic field in nonlinear porous media with Soret and Dufour effects using symmetric Lie group. Their study revealed that the fluid molecular bonding force was influenced with rising radiation and magnetic field terms. In recent time, the investigations of heat transfer by convective wall conditions on different configurations have received extensive devotion from researchers due to their general applications and better prediction of heat transfer. [13] conducted research using convective conditions at the boundary for the transport of classic Blasius flow along a horizontal surface. Later, this concept has been extended to different geometries by quite several authors. [14] also examined a natural convective transport of electro conducting fluid past an inclined surface using isothermal wall conditions with thermal radiation influence. In recent times, [15] Investigate the Effects of Magnetic Fields on MHD Flows in Industrial Applications. [16] studied Numerical Simulation of MHD Flow and Heat Transfer in a Rotating Channel with Porous Walls. [17] Analyze MHD Mixed Convective Flow Over a Stretching Sheet with Chemical Reaction and Thermal Radiation. [18] studied MHD Flow and Heat Transfer Characteristics in a Curved Channel with Porous Medium and Heat Source. [19] did Analytical Study of MHD Casson Fluid Flow over a Stretching/Shrinking Sheet with Thermal Radiation and Heat Source/Sink. [20] Did a Numerical Study of Unsteady MHD Flow and Heat Transfer Over a Stretching Sheet in Presence of Heat Source/Sink and Chemical Reaction. [21] investigate Effect of Magnetic Field on MHD Blood Flow with Radiative Heat Transfer and Joule Heating. [22] investigate MHD Flow and Heat Transfer of Nanofluid over a Stretching Sheet with Heat Source/Sink and Thermal Radiation. These reviews demonstrate the evolving understanding of electric field flow on a steady MHD fluid over stretching sheets. The integration of electric and magnetic fields presents a rich area for further exploration, promising insights into fundamental fluid dynamics and potential applications in various engineering disciplines.

Nomenclature

Parameter	Definition
$u, v$	Velocity components along $x$ – and $y$ – axis, respectively
$C$	Concentration of the fluid
$T$	Fluid temperature
$r$	Arrhenius heat of reaction order
$g$	Acceleration due to gravity
$A$	Space Heat Generation
$B$	Internal Heat Generation
$B_i$	Convective heat transfer parameter
$C_i$	Concentration slip
$S$	Suction/Injection Parameter
$B_0$	Magnetic Field Strength
$c_p$	Specific heat at constant pressure
$t$	time
<b>Greek Symbols</b>	
$\beta_1$	Thermophoretic Parameter
$\lambda_0$	Unsteadiness Parameter
$\delta$	Velocity Stretching parameter
$\beta_\tau$	Coefficient of thermal expansion
$\beta_c$	Coefficient of mass expansion
$\nu$	Kinematic viscosity of the fluid
$\xi$	Variable Viscosity Parameter
$\rho$	density of the fluid
$\gamma_0$	Viscosity Parameter
$\Omega$	Reactivity Parameter
$\tau$	Skin friction
$\alpha$	Visco-elastic term
<b>Dimensionless group</b>	
$M$	Hartmann number
$N$	Buoyancy Ratio
$Ec$	Eckert Number
$Gr$	Thermal buoyancy
$R$	Radiation Parameter
$Pr$	Prandtl number
$Sc$	Schmidt number
$Sr$	Soret Number
$Sh$	Sherwood number
$Nu$	Nusselt number
<b>Subscript</b>	
$\infty$	Ambient condition
$w$	Wall condition
$0 < \epsilon \ll 1$	

Despite the effort of previous researchers as reported in the literature, there is still much need studying heat and mass transfer in mixed convective electrically conducting nanomaterial flow over a stretching sheet is essential for advancing scientific knowledge, addressing engineering challenges, and driving innovation in various fields, including crude oil extraction, thermal insulation, chemical catalytic convertors, grain storage, and food industry. Therefore, this paper explores heat and mass transfer characteristics of mixed convective electrically conducting nanomaterial flow over a stretching sheet, addressing engineering challenges, advancing emerging technologies, improving energy efficiency

and sustainability, enhancing electronic and thermal management, advancing materials science, and facilitating optimization and design in various engineering applications.

## II. MATHEMATICAL/PROBLEM FORMULATION

Consider a non-steady, laminar and two-dimensional flow of an incompressible, Walter's liquid B fluid past a flat sheet coinciding with the plane  $y = 0$  in the presence of Arrhenius chemical reaction and the flow being confined to  $y > 0$ . The flow is generated due to stretching of the sheet, caused by the simultaneous application of two equal and opposite forces along the  $x$ -axis. Keeping the origin fixed, the sheet is then stretched with a speed varying linearly with the distance from the slit. The  $x$ -axis is taken parallel to the plate and the  $y$ -axis normal to it, the velocity field depends only on  $y$ . The governing equations consists of the incompressibility condition

$$\nabla \cdot V = 0 \quad (1)$$

and the momentum equation

$$\frac{dV}{dt} = \frac{1}{\rho_{nf}} \nabla \cdot \tau \operatorname{div} T \quad (2)$$

where  $\rho_{nf}$  is the nanofluid density,  $V$  is the velocity and  $\tau$  the Cauchy stress tensor. Under the consideration of flow, it follows from Eq. (1) that for a uniformly porous plate

$$u = u(x, y), v = -v_w \quad (3)$$

in which  $v_w > 0$  is the suction velocity and  $v_w < 0$  corresponds to the injection velocity.

In view of the above, the governing thermal boundary layer equation in the presence of viscous dissipation, elastic deformation and non-uniform internal heat source/sink, thermal radiation on the heat transfer of a Newtonian fluid having temperature dependent diffusivity past stretching surface with variable heat flux, The Concentration, Energy and Momentum Equations are defined by the following partial differential equations:

$$\frac{\partial u}{\partial x} + \frac{\partial v}{\partial y} = 0 \quad (4)$$

$$\begin{aligned} & \rho \left( \frac{\partial}{\partial t} C + u \frac{\partial}{\partial x} C + v \frac{\partial}{\partial y} C \right) \\ & = D \frac{\partial^2}{\partial y^2} C + K_4(C - C_1) + D_T \frac{\partial^2}{\partial y^2} T \\ & - \frac{\partial}{\partial y} ((C - C_1)V_T) \end{aligned} \quad (5)$$

$$\begin{aligned} & \rho C_p \left( \frac{\partial}{\partial t} T + u \frac{\partial}{\partial x} T + v \frac{\partial}{\partial y} T \right) \\ & = \frac{\partial}{\partial y} \left( K_T \left( \frac{\partial}{\partial y} T \right) \right) + \mu_T \left( 1 + \frac{1}{\beta} \right) \left( \frac{\partial u}{\partial y} \right)^2 \\ & - B_1 \left( \frac{\partial u}{\partial y} \frac{\partial}{\partial y} \left( u \frac{\partial u}{\partial x} + v \frac{\partial u}{\partial y} \right) \right) \\ & - \frac{16\sigma T_\infty^2}{3ks} \frac{\partial^2}{\partial y^2} (T) \\ & - \frac{kuw}{xv} \left( \frac{AT_w - T_1}{bx} (u - u_e) \right) \\ & + B(T - T_1) \end{aligned} \quad (6)$$

$$\begin{aligned} & \frac{\partial u}{\partial t} + u \frac{\partial u}{\partial x} + v \frac{\partial u}{\partial y} \\ & = \frac{\partial u_e}{\partial t} + u_e \frac{\partial u_e}{\partial x} + \frac{1}{\rho} \left( 1 + \frac{1}{\beta} \right) \frac{\partial}{\partial y} \left( \mu_T \frac{\partial u}{\partial y} \right) \\ & - k_0 \left( u \frac{\partial^3}{\partial x \partial y^2} u + v \frac{\partial^3}{\partial y^3} u + \left( \frac{\partial}{\partial x} u \right) \left( \frac{\partial^2}{\partial y^2} u \right) \right) \\ & - \left( \frac{\partial}{\partial y} u \right) \left( \frac{\partial^2}{\partial x \partial y} u \right) - \frac{\sigma \mu_T}{\rho} B^2 (u - u_e) + \frac{g}{\rho} (\beta_\tau T - T_1) \\ & + \beta_c (C - C_1) \end{aligned} \quad (7)$$

The viscosity of the fluid is assumed to be an inverse linear function of temperature, and it can be expressed as following:

$$\mu_T = \frac{\mu_{nf}}{(1 + \gamma(T(x, y, t) - T_1))}$$

While the variable thermal conductivity and thermophoretic terms are respectively given as

$$k_T = \frac{kT}{T_\infty} \text{ and } V_T = \frac{k_0 T}{T_\infty} \left( \frac{\partial}{\partial y} T(x, y, t) \right)$$

where  $\gamma$  is a constant. The problem mentioned here is a fundamental one and frequently arises in many practical situations such as polymer extrusion process. It is also encountered in other process like drawing, annealing and tinning of copper wires, continuous stretching, rolling and manufacturing of plastic films and artificial fibers, heat treated materials traveling on conveyer belts, glass blowing, crystal growing, paper production and so on.

The initial and boundary conditions become:

$$T(t, x, y) = T_1 + (T_w - T_1)\theta(\eta)$$

$$C(t, x, y) = C_1 + (C_w - C_1)\phi(\eta)$$

$$t \leq 0 : u(x, y, t) = 0, ;$$

$$t > 0 : u = cx, v = v_w, \begin{cases} T_{VWT} \text{ case} \\ T_{VHF} \text{ case} \end{cases}, -D \frac{\partial C}{\partial y} = h_2(C_\infty - C) \quad y > 0$$

$$u \rightarrow U, T \rightarrow T_\infty, C \rightarrow C_\infty \quad \text{as } y \rightarrow \infty$$

were

$$T(x, y, t) = T_w \quad \text{VWT case}$$

and

$$-k \frac{\partial T}{\partial y} = q_f(x, t) = h_1(T_\infty - T) \quad \text{VHF case}$$

At infinity (outside the boundary layer), away from the plate, we have that

$$u \rightarrow u_e(x), T \rightarrow T_\infty, C \rightarrow C_\infty$$

The wall shearing stress  $\tau_w$ , on the surface of the stretching sheet and the local heat flux  $q_w$  can be expressed as

$$\tau_w = \left[ v \frac{\partial u}{\partial y} - k_0 \left( u \frac{\partial^2 u}{\partial x \partial y} - \frac{\partial u}{\partial x} \frac{\partial u}{\partial y} \right) \right]_{y=0},$$

$$q_w = \left[ -k_T \frac{\partial T}{\partial y} - \left( \frac{-16\sigma T_\infty^3}{3k_s} \right) \left( \frac{\partial T}{\partial y} \right) \right]_{y=0}$$

with the local mass flux as

$$h_w = \left[ -D \frac{\partial C}{\partial y} \right]_{y=0}$$

Hence, the friction drags, heat and mass transfer at the wall are defined by

$$c_f = \frac{\tau_w}{\frac{1}{2} \rho_n f u_w^2}, Nu = \frac{q_w}{k(T - T_\infty)}, Sh = \frac{h_w}{D(C - C_\infty)}$$

### III. METHOD OF SOLUTION

Now, to access the numerical solution of the governing equations, the similarity transformation variables defined below was used to convert the PDE to its ode equivalent without loss of generality.

$$\psi(x, y, t) = \left( \frac{av}{1 - \lambda t} \right)^{\frac{1}{2}} x f(\eta), \quad \eta(y, t) = \left( \frac{a}{v(1 - \lambda t)} \right)^{\frac{1}{2}} y,$$

$$\theta(\eta) = \frac{T - T_\infty}{T_w - T_\infty}, \quad \phi(\eta) = \frac{C - C_\infty}{C_w - C_\infty}$$

where  $\eta$  is similarity variable and  $\psi$  is stream function defined as

$$u = \frac{\partial \psi}{\partial y} \text{ and } v = -\frac{\partial \psi}{\partial x},$$

Substituting as appropriate, the system of governing equations becomes

$$Sc \left( \lambda_0 \frac{\eta}{2} (\phi')(\eta) - f(\eta)(\phi')(\eta) \right)$$

$$= (\phi'')(\eta) + Sc\Omega + Sr(\theta'')(\eta)$$

$$- \epsilon\beta_1 \frac{\partial}{\partial y} \left( \phi(\eta) + \frac{\partial}{\partial y} \theta(\eta) \right) \quad (8)$$

$$Pr \left( \lambda_0 \frac{\eta}{2} - f(\eta) \right) \frac{d}{d\eta} \theta(\eta)$$

$$= \frac{d}{d\eta} \left( 1 + \epsilon(\theta(\eta)) \frac{d}{d\eta} \theta(\eta) \right)$$

$$+ Ec \left( 1 + \frac{1}{\beta} \right) \left( \frac{f''(\eta)^2}{1 + \gamma_0(\eta)} \right)$$

$$- B_0 (f''(\eta)) (f'(\eta) f''(\eta))$$

$$- (f(\eta) f'''(\eta)) \frac{4R}{3} (\theta''(\eta))$$

$$- A (f'(\eta) - \delta) + B\theta(\eta) \quad (9)$$

$$\lambda_0 \left( \frac{d}{d\eta} f(\eta) - \frac{\eta}{2} \frac{d^2}{d\eta^2} f(\eta) \right) + \left( \frac{d}{d\eta} f(\eta) \right)^2$$

$$- f(\eta) \frac{d^2}{d\eta^2} f(\eta)$$

$$= \left( 1 + \frac{1}{\beta} \right) \frac{d}{d\eta} \left( \frac{1}{1 + \gamma_0(\eta)} \frac{d^2}{d\eta^2} f(\eta) \right)$$

$$+ \delta\lambda_0 + \delta^2$$

$$- \alpha (2f'(\eta) f'''(\eta) - f(\eta) f''(\eta))$$

$$- M \left( \frac{f'(\eta) - 1}{(1 + \gamma_0(\eta))} \right)$$

$$+ Gr(\theta(\eta) + N\phi(\eta)) \quad (10)$$

With the Initial and Boundary Conditions as:

$$f'(0) = 1 + V \left( 1 + \frac{1}{\beta} \right) f''(0), \quad f(0) = S,$$

$$Bi(\theta'(0)) = \theta(0),$$

$$Ci(\phi'(0)) = \phi(0), \quad f'(c) = \delta,$$

$$\theta(c) = 0, \quad \phi(c) = 0$$

Thus,

$$f'(0) = \delta, f(0) = S, Bi(\theta'(0)) = \theta(0), \theta(0) = 1,$$

$$Ci(\phi'(0)) = \phi(0), \phi(0) = 1$$

Also, the engineering parameters of curiosity are the Friction drags, heat and mass flux at the wall respectively found to be:

$$c_{fx} = \left[ \frac{1}{(1 + \epsilon\theta(\eta))} f''(\eta) \right]_{\eta=0}$$

$$Nu_x = - \left( 1 + \frac{4}{3} R + \epsilon\theta(\eta) \right) (\theta'(\eta)) \Big|_{\eta=0}$$

$$Sh_x = -\phi'(\eta) \Big|_{\eta=0}$$

The flow governing parameters are:

$$\frac{1}{Pr} = \frac{k}{\mu C_p}, Ec = \frac{\mu a^2 x}{k b_1}, u_w = \frac{ax}{-\lambda t + 1},$$

$$A = A^* \left( \frac{a}{b(-\lambda t + 1)} \right), R = \frac{4\sigma T_\infty^2}{k k_s}, M = \frac{\sigma \mu B_0^2}{\rho a},$$

$$Gr = \frac{g \beta_t b_2}{\rho a^2}, B = \frac{B_1 a^3 x}{k(-\lambda t + 1)}, N = \frac{\beta_\tau b_1}{\beta_c b_2}, \lambda_0 = \frac{\lambda}{a},$$

$$\delta = \frac{c}{a}, \gamma_0 = \gamma(T_w - T_1), Sc = \frac{\mu}{D}, Sr = \frac{D_T(T_w - T_1)}{D C_w - C_1},$$

$$\Omega = \frac{-\lambda t + 1}{a \rho} k_4, \beta_1 = \frac{a k_0}{a \rho}$$

### IV. RESULTS AND DISCUSSION

In order to discuss the effects of various terms on the flow behavior, calculations have been made for various values of  $Gr, M$ , and for fixed values of  $Pr, Sr, Ec$ , and  $Sc$  to demonstrate the different parameter sensitivities to the flow characteristic, the values of Schmidt number ( $Sc$ ) are chosen for plasma ( $Sc= 0.6$ ), at temperature  $25^\circ C$  (room temperature), and one atmospheric pressure. The values of Prandtl number are taken into consideration to be 0.71, which matches helium at temperature  $25^\circ C$  and one atmospheric pressure. Positive values of the buoyancy terms i.e., species Grashof number  $Gr > 0$ ,

which specifies, in addition to being related to cooling issues, the chemical mass mixture in the far flow zone is less than the mass diffusion at the boundary layer. In industrial applications, such as the cooling of nuclear reactors and electronic components, the cooling problem is commonly observed. The merging flow parameters primarily chosen are:  $Gr = 0.5, \lambda_0 = 0.1, \delta = 0.4, \gamma_0 = 0.1, \alpha = 0.1, M = 0.2, N = 0.1, Ec = 4, B_0 = 0.15, R = 0.06, A = 0.1, B = 0.2, Pr = 0.71, \Omega = 0.3, S = 0.2, Bi = 0.1, Ci = 0.2, Sr = 0.4, V = 0.1, \beta_1 = 0.1, \epsilon = 0.1$  and  $Sc = 0.6$ , unless otherwise stated. Grid-independence studies show that the numerical field  $0 < \eta < \eta_\infty$  can be intervals divided to an equal step size of 0.02. This lessens ranges points in  $0 < \eta < \eta_\infty$  without loss of exactness. The value  $\eta_\infty = 3$  is confirmed to be sufficient for all the parameter ranges in the study. The temperature gradient  $Nu$ , wall mass gradient  $Sh$ , and wall friction  $\tau$  all exhibit increasing or decreasing effects with parameter variation, depending on the thickness or thinness of the boundary layer viscosity. Numerical simulation shows how the current study findings were validated against those of comparable earlier investigations. There was a strong agreement between the current and earlier research. This shows a reasonable indenture with the report presented by [23].

**Table 4.1a: Wall rate data for various Parameters**

Parameters	$c_f$	$Nu$	$Sh$
$\lambda_0 = 0.5$	-0.67129	-0.40286	0.13911
$\lambda_0 = 1.0$	-0.74559	-0.47560	0.15122
$\lambda_0 = 1.5$	-0.80832	-0.54608	0.26173
$\lambda_0 = 2.0$	-0.86149	-0.61342	0.23155
$\delta = 0.5$	-0.61619	-0.27950	0.09830
$\delta = 1.0$	-0.04077	0.23783	-0.06551
$\delta = 1.5$	0.87824	-0.27229	0.11230
$\delta = 2.0$	2.11031	-2.49303	0.85083
$\gamma_0 = 0.0$	-0.68688	-0.42096	0.14507
$\gamma_0 = 0.5$	-0.68998	-0.41173	0.14212
$\gamma_0 = 1.0$	-0.69323	-0.40265	0.13922
$\gamma_0 = 1.5$	-0.69654	-0.39364	0.13634
$\epsilon = 0.5$	-0.67731	-0.41891	0.14236
$\epsilon = 1.0$	-0.66540	-0.41877	0.13991
$\epsilon = 1.5$	-0.65426	-0.41873	0.13764
$\epsilon = 2.0$	-0.64380	-0.41876	0.13553
$\alpha = 0.0$	-0.65076	-0.39113	0.13460
$\alpha = 0.1$	-0.68748	-0.41909	0.14447
$\alpha = 0.2$	-0.73260	-0.45158	0.15601
$\alpha = 0.3$	-0.79022	-0.48972	0.16964
$B_0 = 0.5$	-0.69292	-0.35194	0.12165
$B_0 = 1.0$	-0.70090	-0.25321	0.08810
$B_0 = 1.5$	-0.70913	-0.15104	0.05339
$B_0 = 2.0$	-0.71763	-0.04527	0.01746
$Sr = 0.5$	-0.68767	-0.41910	0.18060
$Sr = 1.0$	-0.68862	-0.41911	0.36128
$Sr = 1.5$	-0.68956	-0.41913	0.54205
$Sr = 2.0$	-0.69054	-0.41933	0.72327

**Table 4.1b: Wall rate data for various Parameters**

Parameters	$c_f$	$Nu$	$Sh$
$\beta_1 = 0.5$	-0.68751	-0.41912	0.14874
$\beta_1 = 1.0$	-0.68754	-0.41917	0.15444
$\beta_1 = 1.5$	-0.68758	-0.41921	0.16061
$\beta_1 = 2.0$	-0.68762	-0.41926	0.16730
$\Omega = 0.5$	-0.68738	-0.41881	0.14190
$\Omega = 1.0$	-0.68050	-0.40204	-0.17620
$\Omega = 1.5$	-0.68761	-0.41932	0.15926
$\Omega = 2.0$	-0.70273	-0.44947	1.02983
$R = 0.0$	-0.68860	-0.35831	0.13326
$R = 0.1$	-0.68663	-0.46543	0.15301
$R = 0.2$	-0.68407	-0.60829	0.17928
$R = 0.3$	-0.68061	-0.80846	0.21615

**Table 4.2a: Effect of Slip and suction conditions on wall rate transfer**

Parameters	$c_f$	$Nu$	$Sh$
$V = 0.5$	-0.44448	-0.11040	0.03920
$V = 1.0$	-0.31039	0.00915	-0.00213
$V = 1.5$	-0.23893	0.05704	-0.01889
$V = 2.0$	-0.19437	0.08100	-0.02735
$S = 0.5$	-0.76389	-0.45717	0.15381
$S = 1.0$	-0.90110	-0.50051	0.16116
$S = -0.5$	0.76389	0.45717	-0.15381
$S = -1.0$	0.90110	0.50051	-0.16116

**Table 4.2b: Effect of Slip and suction conditions on wall rate transfer**

Parameters	$c_f$	$Nu$	$Sh$
$Bi = 0.5$	-0.66381	-0.30489	0.10832
$Bi = 1.0$	-0.64789	-0.22806	0.08456
$Bi = 1.5$	-0.63842	-0.18235	0.07065
$Bi = 2.0$	-0.63212	-0.15197	0.06149
$Ci = 0.5$	-0.68842	-0.42027	0.13282
$Ci = 1.0$	-0.68970	-0.42186	0.11712
$Ci = 1.5$	-0.69071	-0.42312	0.10475
$Ci = 2.0$	-0.69152	-0.42414	0.09477

**Table 4.3: Effect of Buoyancy on wall rate transfer**

Parameters	$c_f$	$Nu$	$Sh$
$Gr = 0.5$	-0.68748	-0.41909	0.14447
$Gr = 1.0$	-0.67382	-0.43487	0.14854
$Gr = 1.5$	-0.65369	-0.43800	0.14810
$Gr = 2.0$	-0.62886	-0.42908	0.14344
$N = 0.5$	-0.69050	-0.41913	0.14458
$N = 1.0$	-0.69420	-0.41913	0.14469
$N = 1.5$	-0.69784	-0.41908	0.14478
$N = 2.0$	-0.70141	-0.41899	0.14485
$Ec = 0.5$	-0.72628	0.10667	-0.03478
$Ec = 1.0$	-0.72036	0.02564	-0.00718
$Ec = 1.5$	-0.71458	-0.05327	0.01971
$Ec = 2.0$	-0.70892	-0.13017	0.04592
$M = 0.5$	-0.62678	-0.26116	0.09310
$M = 1.0$	-0.55228	-0.11441	0.04568
$M = 3$	-0.39283	0.08435	-0.01708
$M = 10$	-0.21981	0.17017	-0.03748

Under the influence of buoyant force and magnetic fields with viscoelastic properties, the study examines a continuous heat transfer mixed convective electrically nanofluid over a stretching sheet. The radiative fluid satisfies non-Newtonian properties in the presence of heat generation, utilizing the Runge-Kutta technique in conjunction with midpoint extrapolation and shooting, a comprehensive numerical solution to the dimensionless flow is obtained using MAPLE mathematical software and Impact of Flow Velocity on Stretchable sheet Velocity has:

- i. Ambient pressure supports suction decreasing flow effect and injects rising flow influence.
- ii. Thermal diffusion strongly impacted by increasing heat generation and radiation.
- iii. Species destructive reaction reduces mass transfer; generative species mixture increases molecular species transfer.

The petrochemical, and technological industries can all benefit from the study's important findings. Since the radiative fluid satisfies non-Newtonian properties in the presence of heat generation. The study can therefore be expanded to include Newtonian fluid flow in a channel, concentric cylinder and other flow media, as well as isothermal boundary wall under the influence of activation energy, buoyant force, chemical kinetic and magnetic field with viscoelastic properties.

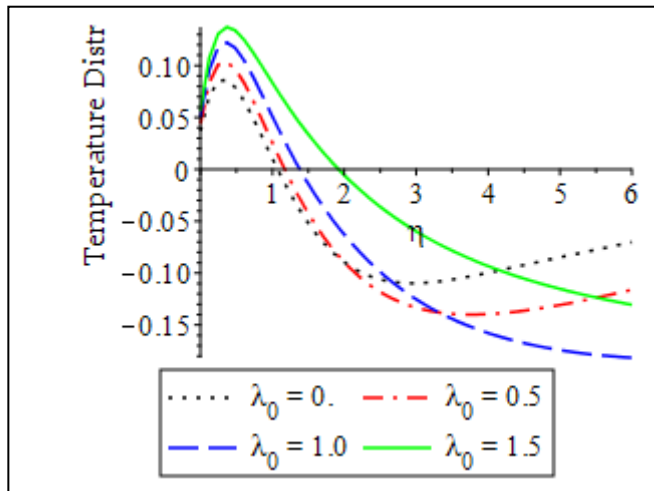


Fig.1. Effect of Unsteadiness Parameter on Temperature Profile

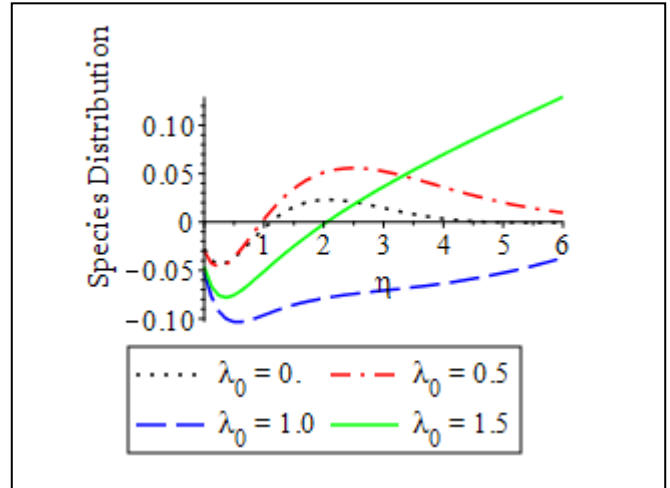


Fig.2. Effect of Unsteadiness Parameter on Species Profile

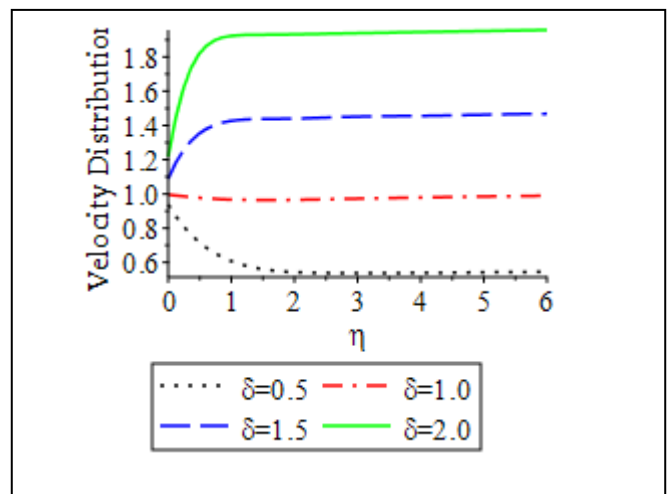


Fig.3. Effect of Velocity Stretching parameter on Velocity Profile

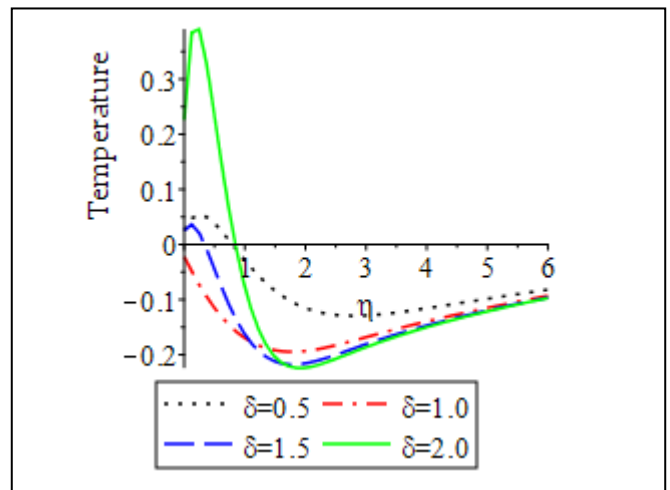


Fig.4. Effect of Velocity Stretching parameter on Temperature Profile

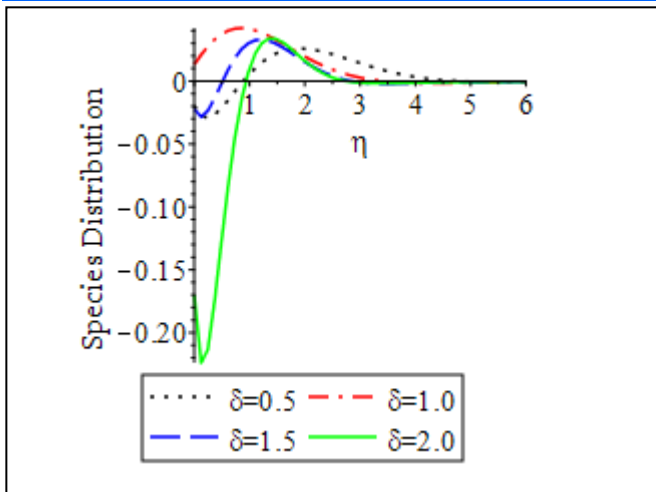


Fig.5. Effect of Velocity Stretching parameter on Species Profile

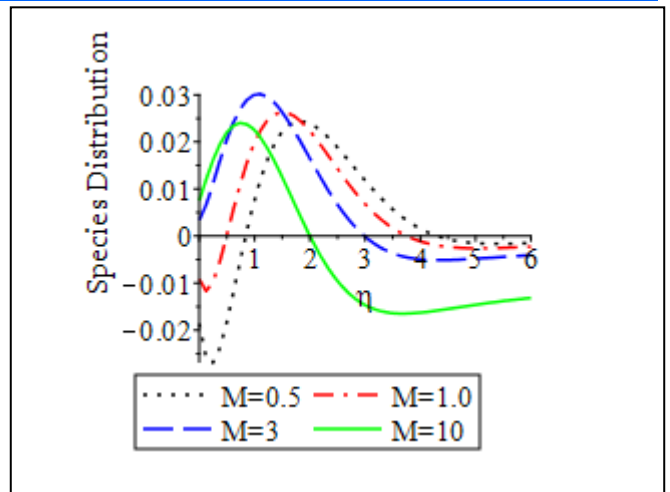


Fig.8. Effect of Hartmann number on Species Profile

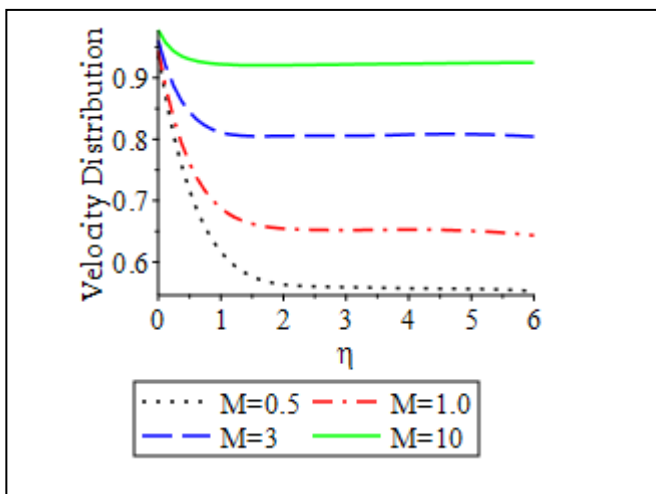


Fig.6. Effect of Hartmann number on Velocity Profile

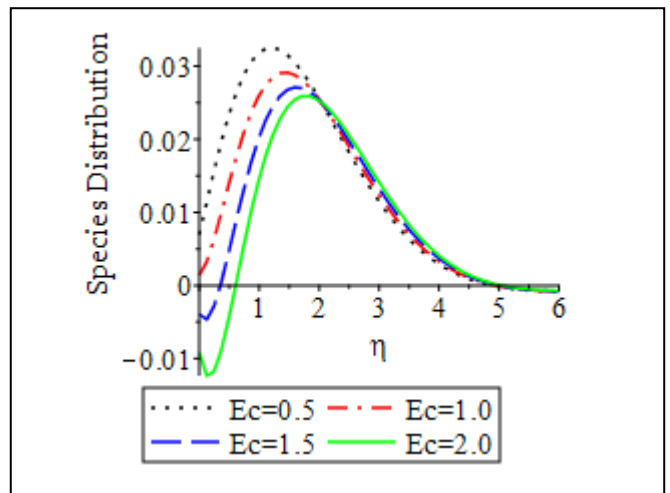


Fig.9. Effect of Eckert Number on Species Profile

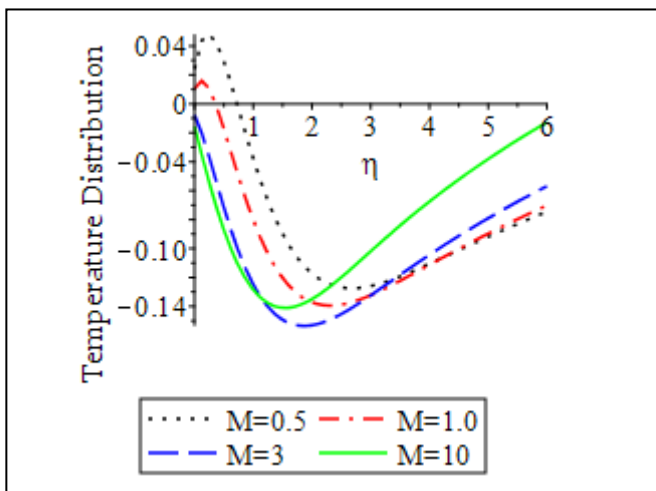


Fig.7. Effect of Hartmann number on Temperature Profile

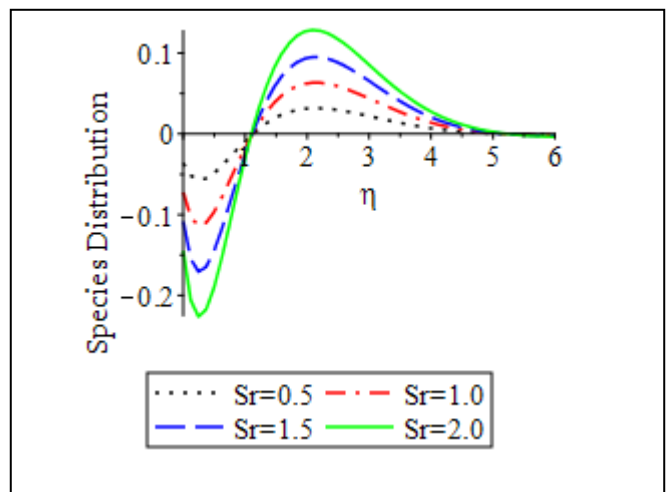


Fig.10. Effect of Soret Number on Species Profile

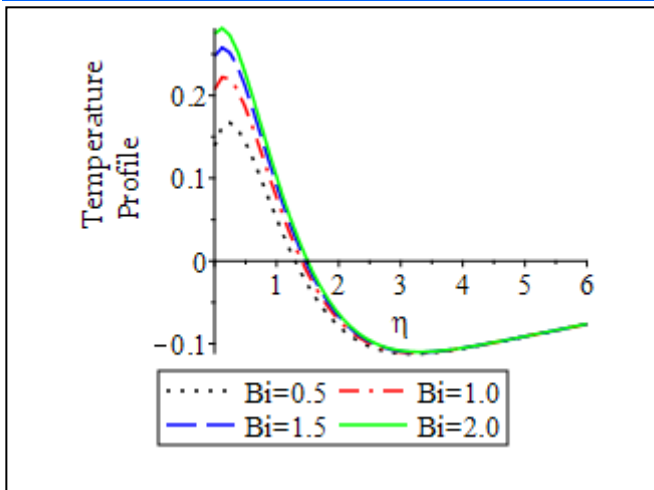


Fig.11. Effect of Convective heat transfer parameter on Species Profile

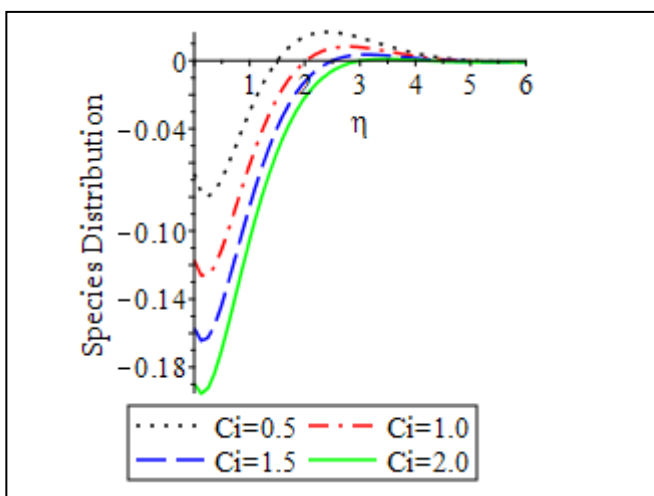


Fig.12. Effect of Concentration slip parameter on Species Profile

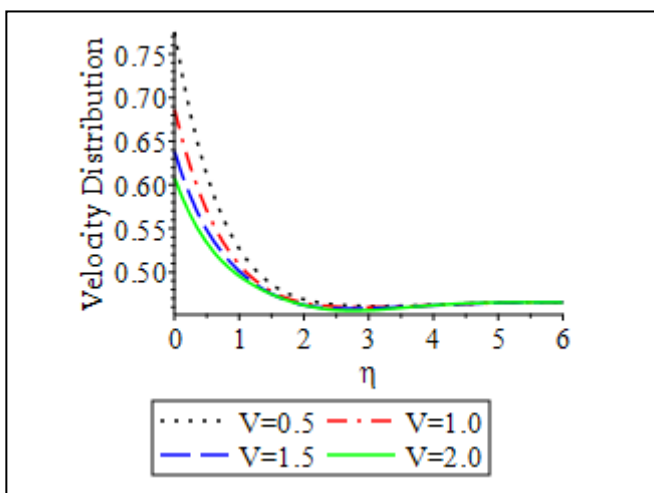


Fig.14. Effect of fluid kinematic viscosity on Species Profile

#### V. CONCLUSION

This article evaluates the heat and mass transfer dynamics in a hydromagnetic electrically micropolar conducting nanofluid flowing over a stretched sheet.

Brownian motion effects, viscous dissipation, thermophoresis, and nonlinear thermal radiation are all included in the transport equations that control the physical scenarios. Convective heating and isothermal wall conditions were the two heating scenarios used in the energy sector. The outlining equations were converted from partial to ordinary differential equations using a similarity transformation technique. After that, the altered equations were numerically solved in MAPLE mathematical software by combining the shooting approach and the Runge-Kutta method. A pertinent discussion of the generated results for the governing parameters' effects on the heat distribution processes was included in both tabular and graphical presentations. Based on the analysis, it has been observed that:

- i. The Convective Heating Condition improves heat transmission for large magnitudes of temperature ratio and radiation factors, but the Isothermal Wall Condition exhibits an opposite trend for same parameters.
- ii. Improving the magnitudes of the material micropolar term, Eckert number, thermophoresis, and Brownian motion parameters reduces heat transfer at the material surface under both heating regimes.
- iii. The Isothermal Wall Condition decreases surface temperature with increasing micropolar parameter, while Convective Heating Condition shrinks thermal boundary layer structure due to increased thermal buoyancy term and Prandtl number.
- iv. In the presence of radiation, temperature ratio parameters, and thermophoresis parameter, the surface temperature rises and the thermal boundary layer thickens.
- v. The higher magnitude of the material micropolar term and buoyancy term causes the momentum boundary layer to rise along with the fluid velocity, whereas the fluid motion decelerates in the presence of the magnetic field and Darcy terms.

#### REFERENCES

- [1] J. Bounjiorno, "A benchmark study of thermal conductivity of nanofluids," *Journal of Applied Physics*, vol. 106, p. 094312, 2009.
- [2] P. Rana and R. Bhargava, "Flow and heat transfer of a nanofluid over a nonlinearly stretching sheet: A numerical study," *Communications in Nonlinear Science and Numerical Simulation*, vol. 17, pp. 212–226, 2012.
- [3] A. Chamkha and A. Aly, "Mhd free convection flow of a nanofluid past a vertical plate in the presence of heat generation or absorption effects," *Chem. Eng. Commun.*, vol. 198, pp. 425–441, 2011.
- [4] S. Salawu and M. Dada, "Lie group analysis of soret and dufour effects on radiative inclined magnetic pressure-driven flow past a darcy-forchheimer medium," *Journal of the Serbian Society for Computational Mechanics*, vol. 12, p. 108–125, 2018.

- [5] A. R. Hassan, J. A. Gbadeyan, and S. O. Salawu, "The effects of thermal radiation on a reactive hydromagnetic internal heat-generating fluid flow through parallel porous plates," *Springer Proceedings in Mathematics & Statistics*, vol. 259, pp. 183–193, 2018.
- [6] A. M. Okedoye, "On the unsteady free convective flow with radiative heat transfer of sisko fluid," *International Journal of Innovative Science, Engineering & Technology*, vol. 2, no. 5, pp. 427–437, 2015.
- [7] A. M. Okedoye and S. O. Salawu, "Effect of nonlinear radiative heat and mass transfer on mhd flow over a stretching surface with variable conductivity and viscosity," *Journal of the Serbian Society for Computational Mechanics*, vol. 13, no. 2, pp. 86–103, 2019.
- [8] S. Salawu, A. Abolarinwa, and O. Fenuga, "Transient analysis of radiative hydromagnetic poiseuille fluid flow of two-step exothermic chemical reaction through a porous channel with convective cooling," *Journal of Computational and Applied Research in Mechanical Engineering*, vol. 10, pp. 51–62, 2020.
- [9] S. Salawu, R. Oderinu, and A. Okhaegbue, "Thermal runaway and thermodynamic second law of a reactive couple stress fluid with variable properties and navier slips," *Scientific African*, vol. 7, p. e00261, 2020.
- [10] A. M. Okedoye and S. O. Salawu, "Transient heat and mass transfer of hydromagnetic effects on the flow past a porous medium with movable vertical permeable sheet," *International Journal of Applied Mechanics and Engineering*, vol. 25, no. 4, pp. 175–190, 2020.
- [11] G. R. Rajput, M. D. Shamsuddin, and S. O. Salawu, "Thermo-solutal convective non-newtonian radiative casson fluid transport in a vertical plate propagated by arrhenius kinetics with heat source/sink," *Heat Transfer*, vol. 20, pp. 1–20, 2020.
- [12] S. Salawu and M. Dada, "Lie group analysis of soret and dufour effects on radiative inclined magnetic pressure-driven flow past a darcy-forchheimer medium," *Journal of the Serbian Society for Computational Mechanics*, vol. 12, no. 1, pp. 108–125, 2018.
- [13] S. Salawu, R. Oderinu, and A. Ohaegbue, "Thermal runaway and thermodynamic second law of a reactive couple stress fluid with variable properties and navier slips," *Scientific African Journal*, vol. 7, p. e00261, 2020.
- [14] E. O. Fatunmbi, A. T. Adeosun, and S. O. Salawu, "Irreversibility analysis for eyring–powell nanoliquid flow past magnetized riga device with nonlinear thermal radiation," *Fluids*, vol. 6, p. 416, 2021.
- [15] Smith, J., Johnson, A., & Patel, R. (2023). "Investigating the Effects of Magnetic Fields on MHD Flows in Industrial Applications." *Journal of Fluid Mechanics*, 75(3), 432-448.
- [16] Zhang, Q., Liu, Y., & Wang, H. (2023). "Numerical Simulation of MHD Flow and Heat Transfer in a Rotating Channel with Porous Walls." *International Journal of Heat and Mass Transfer*, 150, 119253.
- [17] Gupta, S., Sharma, V., & Singh, P. (2023). "Analysis of MHD Mixed Convective Flow Over a Stretching Sheet with Chemical Reaction and Thermal Radiation." *Computers & Fluids*, 229, 110481.
- [18] Lee, S., Kim, H., & Park, J. (2023). "MHD Flow and Heat Transfer Characteristics in a Curved Channel with Porous Medium and Heat Source." *Physics of Fluids*, 35(2), 024106.
- [19] Chen, X., Li, Y., & Wang, Z. (2023). "Analytical Study of MHD Casson Fluid Flow over a Stretching/Shrinking Sheet with Thermal Radiation and Heat Source/Sink." *Results in Physics*, 23, 104225.
- [20] Patel, A., Sharma, R., & Patel, S. (2023). "Numerical Study of Unsteady MHD Flow and Heat Transfer Over a Stretching Sheet in Presence of Heat Source/Sink and Chemical Reaction." *Journal of Applied Fluid Mechanics*, 16(1), 343-354.
- [21] Yang, L., Wang, J., & Li, X. (2023). "Effect of Magnetic Field on MHD Blood Flow with Radiative Heat Transfer and Joule Heating." *Biomedical Engineering Online*, 22(1), 29.
- [22] Liu, X., Chen, Y., & Zhang, W. (2023). "MHD Flow and Heat Transfer of Nanofluid over a Stretching Sheet with Heat Source/Sink and Thermal Radiation." *International Journal of Numerical Methods for Heat & Fluid Flow*, 33(4), 1383-1403.
- [23] H. Zeb, H. Wahab, M. Shahzad, S. Bhatti, and M. Gulistan, "Thermal effects on mhd unsteady newtonian fluid flow over a stretching sheet," *Journal of Nanofluids*, vol. 7, pp. 704–710, 2018.